Fully bold formalism at strong coupling regime for the $(0+0)$-dimensionnal Hubbard model

Esteban Foucher*
Ecole Normale Supérieure PSL, Paris, France
(Dated: August 26, 2022)

Failure of the standard skeleton series for on-site interacting systems at strong correlation have been observed in the last decade. Work was done to explain this phenomenon that is understood analytically for the (0+0)d Hubbard model. In this study, we decouple the action of this toy model and transpose it to an electron-boson model to implement the fully-bold formalism with dressed fermionic propagator and screened interaction. We show that this expansion allows accessing stronger correlations than the G-bold expansion. We also provide a complex analysis viewpoint of the multiple branching phenomenon appearing in dressed formalisms for the (0+0)d model.

Keywords: strongly correlated electrons, Hubbard interaction, Feynman diagrams, misleading convergence

I. INTRODUCTION

Feynman diagrams allow computing physical quantities of quantum systems as perturbative developpements in their interaction. It has become an essential tool for quantum physicists, as it can be applied to a lot of systems and allows numerical implementations with great precision such as widely used quantum Monte Carlo algorithms. Dressing techniques and resummation techniques in general are at the heart of Feynman diagrams theory. They consist in wisely rearranging the terms of the diagrammatic series to catch the interesting physics of study, increase the order of convergence of the developpement to reduce the number of terms needed, or manage with diverging developpements. It can be of great interest when dealing with strongly correlated systems as we want to access non-trivial physics where pertinent variables can be different than for weakly correlated cases.
Since its introduction in 1963, the Hubbard model has been widely studied as a theoretical laboratory for condensed matter physics. Despite its simple Hamiltonian only including a kinetic term and an on-site repulsion term, it has been used to describe many fermionic physics among which high-temperature superconductivity, quantum magnetism, charge density waves, Mott insulators.

In the last decade, a new light has been shed on the simplest dressing procedure. It consists in computing diagrammatic series only using a certain class of diagrams called irreducible (or skeleton) while replacing the non-interacting Green's function G_0 by the physical Green's function (GF) G. It has been shown in [5] that this dressed formalism could lead to unphysical answers for on-site interactions at strong correlation. From a series viewpoint, we rearrange the order of summation of an infinite number of diagrams which is a priori a forbidden procedure outside the disc of convergence. From a thermodynamic viewpoint, the Luttinger-Ward functionnal $\Phi[G]$ modelling the interaction part of the grand potential Ω is ill-defined. Indeed, we obtain $\Phi[G]$ by Legendre transform but nothing assures the hypothesis of convexity at strong correlation.

Work has been done to study the misleading convergence of this bold formalism. A full analytical description of misleading convergence for the (0+0)-d Hubbard model is provided in [8] and [10]. The striking similarity between results for the (0+0)-d Hubbard model and for the Hubbard atom showing both a physical and an unphysical regime suggests that the phenomenon arises from the algebraic rearranging of diagrams already encoded in the (0+0)-d Hubbard model. This is all the more confirmed by the fact that the Hubbard atom can be modelled by a (0+0)-d Hubbard model with an effective action [4]. In [8] is shown that different types of dressed expansion (ΓG^2) can improve the range of the physical regime.

In this work we apply the fully-bold formalism with screened interaction and physical GF to the (0+0)-d Hubbard model by decoupling the interaction into charge and spin channels. We show it is a promising way to access

* Correspondence email address: esteban.foucher@ens.psl.eu

arbitrary strong correlation.

Section II is a theoretical reminder of concepts used in this study. Next sections focus on the (0+0)-d model. Section III is a quick reminder of previous results that have led to this study, Section IV provides the computation of the fully-bold formalism, section V is a general discussion on dressing with a comlex analysis viewpoint, and section VI shows numerical results obtained for the fully-bold formalism.

II. THEORY

In this section we briefly introduce some concepts and notations for our study. Most of them can be found in introductory books of condensed matter theory. Explanations are non-exhaustive and steps are being skipped but references are provided to the reader.

A. Coherent states

Let us consider a quantum system of identical particles with creation and annihilation operators $\hat{a}_u^\dagger$ and $\hat{a}_u$ where u indices generally denote position, time and spin.
A well-known basis of the Hilbert space are the Fock states $|(\vec{x}_i, t_i, \sigma_i)_i\rangle$ where i denotes each particle of the system. Those states are obtain by iteratively applying $\hat{a}^\dagger_{\vec{x}_i,t_i,\sigma_i}$ to the void $|0\rangle$. This is a useful basis often associated to its conjugate basis in momentum $|(\vec{p}_i, t_i, \sigma_i)_i\rangle$. Those widely used basis physically describe systems of particles with well-defined position (resp. momentum) and number of particle. However by uncertainty principle, they have undefined momentum (resp. position).
Another useful basis of states are coherent states, that can be defined as eigenstates of the annihilation operator $\hat{a}_u$:

$$\hat{a}_u \, |\xi_u\rangle = \xi_u \, |\xi_u\rangle \tag{1}$$

By definition, eigenvalues ξ_u must respect the same commutation relations than operators:

$$[\xi_u, \xi_v]_\mp = 0 \tag{2}$$

For bosons, they are complex fields, for fermions they are Grassmann fields. This basis has the advantage of encoding the symetries of the bosonic/fermionic statistics in their parametrization of the phase space.

More detailed informations on coherent states and Grassmann variables can be found in [6].

B. Path integrals

In the following, we will need to compute the partition function of our system. It is the sum of the probabilities of all quantum states and allows computing physical quantities as moments of the probability law. We recall in the grand canonical ensemble $Z = Tr\left(e^{-\beta\left(\hat{H}-\mu\hat{N}\right)}\right)$. Fock states can be used to compute it:

$$Z = \int dn \, \langle n| \, e^{-\beta\left(\hat{H}-\mu\hat{N}\right)} \, |n\rangle \tag{3}$$

where n is a general notation to parametrize Fock states. For convenience we have set $\hbar = 1$.
In the following however, coherent states will be more suitable :

$$Z = \int d\xi \, \langle \pm\xi| \, e^{-\beta\left(\hat{H}-\mu\hat{N}\right)} \, |\xi\rangle \tag{4}$$

Where the $+$ is for bosons and the $-$ for fermions. Now a way to replace what can be interpreted as a transition amplitude over imaginary time $\langle \pm\xi| \, e^{-\beta\left(\hat{H}-\mu\hat{N}\right)} \, |\xi\rangle$ is to split the time interval in several smaller ones. Indeed

going from the state $|\xi\rangle$ to $|\pm\xi\rangle$ from $t=0$ to $t=i$ can be seen as going from the state $|\xi\rangle$ to $\left|\xi_{i/2}\right\rangle$ in $\Delta t = i/2$ and then to go from $\left|\xi_{i/2}\right\rangle$ to $|\pm\xi\rangle$ in $\Delta t = i/2$, for arbitrary $\left|\xi_{i/2}\right\rangle$:

$$\langle\pm\xi|\, e^{-\beta\left(\hat{H}-\mu\hat{N}\right)}\,|\xi\rangle = \int d\bar{\xi}_{i/2} d\xi_{i/2}\, \langle\pm\xi|\, e^{-\beta/2\left(\hat{H}-\mu\hat{N}\right)}\,\left|\xi_{i/2}\right\rangle \left\langle\xi_{i/2}\right|\, e^{-\beta/2\left(\hat{H}-\mu\hat{N}\right)}\,|\xi\rangle \tag{5}$$

up to a normalization factor. We can repeat the operation to the limit of an infinity of splitting. That is equivalent to say that going from the state $|\xi\rangle$ to $|\pm\xi\rangle$ from $t=0$ to $t=i$ is possible by using all paths starting from $|\xi\rangle$ at $t=0$ and arriving at $|\pm\xi\rangle$ at $t=i$. Each path being assigned a probability weight $e^{-S[\xi(t)]}$ where S is called the action:

$$Z = \int_{\xi(0)=\pm\xi(\beta)} D[\xi_u(t), \bar{\xi}_u(t)] e^{-S[\xi(t)]} \tag{6}$$

$$S = \int_0^\beta \bar{\xi}_u(t) \left(\frac{\partial}{\partial t} - \mu\right) \xi_u(t) + H\left(\bar{\xi}_u(t), \xi_u(t)\right) dt \tag{7}$$

Where $H\left(\bar{\xi}_u(t), \xi_u(t)\right)$ is obtained by taking $H\left(\hat{a}_u^\dagger(t), \hat{a}_u(t)\right)$ and replacing $\hat{a}_u^\dagger$ by $\bar{\xi}_u(t)$ and $\hat{a}_u(t)$ by $\xi_u(t)$. Here the commutation/anticommutation properties of the integration variables respecting those of the operators have been crucial to obtain such a simple expression of Z. More detailed informations on path integrals are in [3, 6, 9]

C. Green's function

We define the single particle Green's function as the matrix which elements are amplitudes of transition between states. Defining the statistical operator :

$$\hat{\rho} = e^{-\beta\left(\hat{H}-\mu\hat{N}\right)} / Tr\left(e^{-\beta\left(\hat{H}-\mu\hat{N}\right)}\right) \tag{8}$$

$$G_{uv} = -Tr[\hat{\rho} T\left(\hat{a}_u \hat{a}_v^\dagger\right)] = -<T\left(\hat{a}_u \hat{a}_v^\dagger\right)> \tag{9}$$

where T is the operator of time ordering and rearranges a group of operators by putting earlier times to the right and later to the left. G can naturally be expressed in a more compact way with ξ variables:

$$G_{uv} = -<\xi_u \bar{\xi}_v> \tag{10}$$

The expression can be read as the creation of a particle in v (operator $\hat{a}_v^\dagger$ or analogous $\bar{\xi}_v$) that propagates and is annihilated in u (operator $\hat{a}_u$ or analogous ξ_u). G is often called propagator and describes how the particle created propagates in the system. In the case we switch off interactions between particles, the resulting GF is called free (or bare) propagator, noted G_0, and represented as an oriented line in the langage of diagrams. In the interacting (and physical) case it is represented as a bold oriented line.

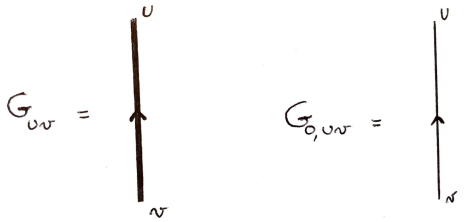

More informations on Green's functions formalism can be found in [2, 6].

D. Feynman diagrams

Most of the time, when particles of our system of study interact, analytical computing of the Green's function and other physical quantities is not possible. We thus need to compute it order by order in interaction $\hat{H}_{int}$ using Feynman diagrams.
Let's have a look at the expression $< T(\hat{A}(\hat{a}_u, \hat{a}_u^\dagger)) >$ for $\hat{A}$ a given operator. This is:

$$\frac{1}{Z}\int_{\varphi(0)=-\varphi(\beta)} D[\varphi_u(t), \bar{\varphi}_u(t)]A(\varphi_u(t), \bar{\varphi}_u(t))e^{-S[\varphi(t)]} \tag{11}$$

we intentionally switched to fermionic systems as this will be our case of study. Now the idea is to split the action $S = S_0 + S_{int}$ where S_0 is the non interacting part of the action and S_{int} contains the interactions. Often, S_0 is bilinear in Grassmann fields and easy to treat while S_{int} is quadratic for two-body interactions. Now the integral has the form:

$$\begin{aligned} < T(\hat{A}(\hat{a}_u, \hat{a}_u^\dagger)) > &= -\frac{\int D[\varphi, \bar{\varphi}]e^{-(S_0+S_{int})}A}{\int D[\varphi, \bar{\varphi}]e^{-(S_0+S_{int})}} \\ &= -\frac{< e^{-S_{int}}A >_0}{< e^{-S_{int}} >_0} \end{aligned} \tag{12}$$

Where $< ... >_0$ stands for statistical average with the non-interacting partition function. We can power now expand the exponential:

$$< e^{-S_{int}}A >_0 = \sum_k < \frac{(-S_{int})^k}{k!}A >_0 = \sum_k < \frac{(-\int d\bar{\varphi}d\varphi H_{int}(\bar{\varphi}, \varphi))^k}{k!}A >_0 \tag{13}$$

Wick's theorem gives us a way to write each term as a product of G_0s and Us. Those resulting term can be represented as diagrams. The linked custer theorem states that only connected diagrams contribute to $-\frac{< e^{-S_{int}}A >_0}{< e^{-S_{int}} >_0}$.
Disconnected diagrams compensate between the numerator and the denominator.
In the case of a two-body interaction, this gives us the diagrammatic expansion of G:

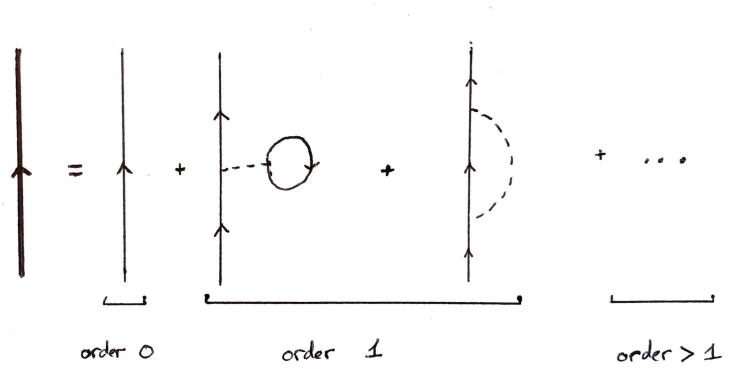

where dashed lines represent the interactions. We only represented diagrams to first order in interaction (only 1 dashed line). Those are called bare diagrams as they involve bare propagators and bare interactions, opposed to full propagators and screened interaction. The equality above is the diagrammatic expression of the relation in the X-coordinates:

$$\begin{aligned} G_{uv} = G_{0,uv} &- \int dX_1 dX_2 G_0(X_u, X_1)_{\sigma_u\sigma_1}U(X_1, X_2)_{\sigma_1\sigma_1',\sigma_2\sigma_2'}G_0(X_1, X_v)_{\sigma_1'\sigma_v}G_0(X_2, X_2)_{\sigma_2'\sigma_2} \\ &+ \int dX_1 dX_2 G_0(X_u, X_1)_{\sigma_u\sigma_2}G_0(X_2, X_1)_{\sigma_2'\sigma_1}U(X_1, X_2)_{\sigma_1\sigma_1',\sigma_2\sigma_2'}G_0(X_1, X_v)_{\sigma_1'\sigma_v} \\ &+ \text{higher orders ...} \end{aligned} \tag{14}$$

Here we quickly exposed the way to introduce diagrams. For more details one can see [2, 6].

E. Dyson's equations and irreducible diagrams

We define the self-energy Σ as verifying Dyson's equation given in its algebraic and diagrammatic form:

$$G_{uv} = G_{0,uv} + G_{0,u\alpha}\Sigma_{\alpha\beta}G_{\beta v} \tag{15}$$

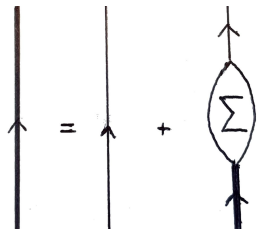

We give here self-energy diagrams at first order:

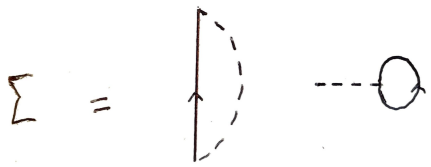

While constructing a bare diagrammatic series, one can absorb all diagrams that can be obtained by inserting a self-energy diagram into the propagator of a diagram of lower order (we say the diagram is reducible). At each order, one can thus replace all bare propagators G_0 by full G while only keeping irreducible diagrams. The skeleton series obtained is equivalent to the bare series at each order in U which is assured by Dyson's equation. In practice, a diagram is irreducible if it is not possible to split it in two disconnected parts by cutting two propagators (Fig. 1). In the following we will use fully-bold diagrams, skeletonized with respect to fermionic propagators and interactions (Fig. 2).

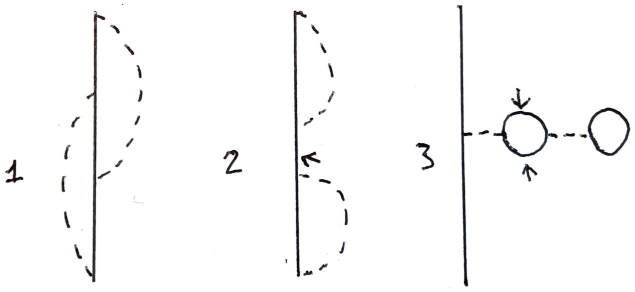

Figure 1. Diagram 1 is irreducible while diagrams 2 and 3 can be split into two parts when removing propagators indicated by arrows.

Figure 2. $W_{\alpha\beta} = U_{\alpha\beta} + U_{\alpha\gamma}\Pi_{\gamma\delta}W_{\delta\beta}$. One can define the polarisation Π, diagrammatic analogous of Σ for the screened interaction (wavy lines). A diagram is irreducible with respect to interactions if it is not possible to split it in two disconnected parts by cutting two interaction lines.

III. PREVIOUS RESULTS ON MISLEADING CONVERGENCE

It has first been shown numerically in [5] that the standard bold formalism (dressed G, bare U) converged to an unphysical answer at strong correlation for the Hubbard atom, the 2D Hubbard model and for the single-site Anderson impurity model. Later the same phenomenon has been analytically described for the (0+0)d Hubbard model [8] while a link between physical and toy model can be made [4].

A. From the Hubbard atom to the (0+0)d Hubbard model

The Hubbard atom models one valence site where there can be 0, 1 or 2 electrons with opposite spins by Pauli exclusion. Its action is :

$$S^{HA} = \frac{U}{2\beta}\sum_{k}\left(\sum_{n\sigma}\bar{\varphi}_{n-k,\sigma}\varphi_{n,\sigma}\right)\left(\sum_{m\sigma'}\bar{\varphi}_{m+k,\sigma'}\varphi_{m,\sigma'}\right) - \sum_{n\sigma}\bar{\varphi}_{n,\sigma}\left(i\omega_n + \mu\right)\varphi_{n,\sigma} \tag{16}$$

where $\omega_n = (2n+1)\pi/\beta$ are the Matsubara frequencies. Its partition function is the integral:

$$Z = \int\prod_{n,\sigma} D[\bar{\varphi}_{n,\sigma}, \varphi_{n,\sigma}]e^{-S^{HA}} \tag{17}$$

In [4] is explained how to model the Hubbard atom with a (0+0)d hubbard model. We can integrate expression (17) over all Matsubara frequencies but one (of indice n). Due to the Grassmann algebra, we end up with an effective action S_{eff} that is only composed of terms up to quartic interactions:

$$\begin{aligned} Z &= \int\prod_{\sigma} D[\bar{\varphi}_{n,\sigma}, \varphi_{n,\sigma}]e^{-S_{eff}} \\ S_{eff} &= U_{eff}\prod_{\sigma}\left(\bar{\varphi}_{n,\sigma}\varphi_{n,\sigma}\right) - \mu_{eff}\sum_{\sigma}\left(\bar{\varphi}_{n,\sigma}\varphi_{n,\sigma}\right) \end{aligned} \tag{18}$$

At half-filling and keeping the lowest frequency (n=1) this gives us:

$$\begin{aligned} U_{eff} &= \frac{\omega_n^2 + U^2/4}{X(n,\beta U/2)} - \frac{\omega_n^2}{X^2(n,\beta U/2)} \\ \mu_{eff} &= \frac{i\omega_n}{X(n,\beta U/2)} \end{aligned} \tag{19}$$

Where X is a real dimensionless real function.

This result makes a clear link between the Hubbard atom and the (0+0)d Hubbard model where interactions between all modes have been grouped into a single effective interaction for the first mode. It sheds a new light on this toy model and provides a physical interpretation of it. This link can partly explain the obvious similarity observed in [8] on the multi-regime phenomenon of bold formalism for the Hubbard atom and the (0+0)d Hubbard model.

B. Results on the (0+0)d Hubbard model

We expose here a quick reminder on the results for the (0+0)d Hubbard model. In this symplified model, diagrams are numbers and the only remaining indices are spins. The partition function is an integral over Grassmann variables:

$$\begin{aligned} Z &= \int \prod_{\sigma} (d\bar{\varphi}_\sigma d\varphi_\sigma)\, e^{G_0^{-1} \sum_\sigma \bar{\varphi}_\sigma \varphi_\sigma - U \bar{\varphi}_\uparrow \varphi_\uparrow \bar{\varphi}_\downarrow \varphi_\downarrow} \\ Z &= G_0^{-2} - U \end{aligned} \tag{20}$$

The Green's function G is given by :

$$\begin{aligned} G_\sigma &= - < \varphi_\sigma \bar{\varphi}_\sigma > \\ G_\sigma \equiv G &= \frac{G_0}{1 - U G_0^2} \end{aligned} \tag{21}$$

In this model, bare diagrammatic series are power series over the scalar variable UG_0^2 while skeleton series are over UG^2. [8] shows a double branch structure of $\Sigma(U, G)$ and a failure of the bold scheme with two clear regimes: a physical regime at low correlation ($|UG_0^2| < 1$) and an unphysical regime ($|UG_0^2| > 1$) at strong correlation. [8] also demonstrates that one can push further the limit of validity of the skeleton series using the fully-bold formalism with single particle propagator G and pair propagator Γ:

$$\begin{aligned} \Gamma &= U - U^2 < \varphi_\uparrow \varphi_\downarrow \bar{\varphi}_\uparrow \bar{\varphi}_\downarrow > \\ &= U \frac{1 - 2UG_0^2}{1 - UG_0^2} \end{aligned} \tag{22}$$

Now the fully dressed series is a power series over the variable ΓG^2 and becomes unphysical for $|UG_0^2| > \frac{1+\sqrt{3}}{2}$. The physical range is wider than previously. This second developpement also has the advantage of improving the convergence of the diagrammatic expansion.
On this observation, one can wonder if another type of diagramamtic series would allow to access a regime of stronger correlation which is a general challenge in condensed matter physics.

IV. HEISENBERG DECOUPLING AND FULLY-DRESSED FORMALISM

As described in [1], we will apply Heisenberg decoupling to the (0+0)d Hubbard model and compute the resulting screened interaction. The idea is to split the total interaction term U into a charge interaction and a spin interaction. This method is general and can be applied to other systems.

A. Heisenberg decoupling

Let us consider the general action for an electronic problem:

$$S = \bar{\varphi}_u [-G_0^{-1}]_{uv} \varphi_v + \frac{U_{uv}}{2} \bar{\varphi}_u \varphi_u \bar{\varphi}_v \varphi_v \tag{23}$$

where indices u and v denote position (or momentum), spin and time (or frequency). In our specific case, the only indices are spins and S reduces to:

$$S = -G_0^{-1} n + U n_\uparrow n_\downarrow \tag{24}$$

Heisenberg decoupling consists in the following equality for Grassmannn fields iff $U = U^{ch} - 3U^{sp}$:

$$U n_\uparrow n_\downarrow = \frac{U^{ch}}{2} nn + \frac{U^{sp}}{2} \vec{s}.\vec{s} \tag{25}$$

We recall that the Grassmann representation of the spin density $s^{i=x,y,z}$ along the i-axis is given by:

$$s^i = \bar{\varphi}_u \sigma^i_{uv} \varphi_v, \ \vec{s}.\vec{s} = (s^x)^2 + (s^y)^2 + (s^z)^2 \tag{26}$$

where σ^i is the i-th Pauli matrix.

Our approach will be to study the general problem with an action of the form:

$$S = -G_0^{-1} n + \frac{U^{ch}}{2} nn + \frac{U^{sp}}{2} \vec{s}.\vec{s} \tag{27}$$

and get back to the initial problem applying the condition:

$$U = U^{ch} - 3U^{sp} \Leftrightarrow U^{ch} = (3\alpha - 1)U \text{ and } U^{sp} = (\alpha - 2/3)U \tag{28}$$

for α an a priori free parameter but that has an influence on the range of validity of the scheme (as we show in section VI). While we had at first an anti-diagonal Hamiltonian in spin indices, we now have a problem with diagonal Hamiltonian in charge and spin channels. In this sense we call the method decoupling.

Another decoupling that we did not have time to treat is Ising decoupling that is only seperating z-axis spin interaction from charge interaction. We decided to use Heisenberg decoupling as it is rotationnal invariant and more physical because it clearly seperates charges and spin interactions. It would nevertheless be interesting to do the computation for Ising decoupling to see how misleading convergence occurs and compare both methods.

B. Computation for Heisenberg decoupling

We consider the more general problem with action:

$$S = -G_0^{-1} n + \frac{U^{ch}}{2} nn + \frac{U^{sp}}{2} \vec{s}.\vec{s} \tag{29}$$

where G_0, U^{ch}, and U^{ch} are independant.

1. Partition function

The partition function is given by the integral over Grassmannn variables:

$$\begin{aligned} Z &= \int d\bar{\varphi}_\uparrow d\varphi_\uparrow d\bar{\varphi}_\downarrow d\varphi_\downarrow e^{-S} \\ Z &= G_0^{-2} - (U^{ch} - 3U^{sp}) \end{aligned} \tag{30}$$

2. Full fermionic propagator

The full fermionic propagator G is given by:

$$G_{\sigma\sigma'} = - < \varphi_\sigma \bar{\varphi}_{\sigma'} > \tag{31}$$

$$G = \delta_{\sigma\sigma'} \frac{G_0}{1 - (U^{ch} - 3U^{sp}) G_0^2} \tag{32}$$

3. Screened interaction

To compute the screened interaction, we introduce a real scalar field via a following Hubbard-Stratonovic transformation. This general transformation's interpretation is that the two-fermions interaction can be seen as the exchange of a fictive boson. The interaction being Hermitian, this boson must be real to preserve symmetry.

$$\begin{aligned}\exp(-S_{int}) &= \exp\left(-\frac{U^{ch}}{2}nn - \frac{U^{sp}}{2}\vec{s}.\vec{s}\right) \\ &= \int D[\phi]\exp\left(\frac{(U^{ch})^{-1}}{2}\phi_{ch}^2 + \frac{(U^{sp})^{-1}}{2}\vec{\phi}_{sp}.\vec{\phi}_{sp} + \phi_{ch}n + \vec{\phi}_{sp}.\vec{s}\right)\end{aligned} \tag{33}$$

The partition function is now given by the integral over Grassmann and scalar variables:

$$Z = \int D[\phi]D[\bar{\varphi},\varphi]\exp\left(\frac{(U^{ch})^{-1}}{2}\phi_{ch}^2 + \frac{(U^{sp})^{-1}}{2}|\vec{\phi}_{sp}|^2 + (G_0^{-1}+\phi_{ch})n + \vec{\phi}_{sp}.\vec{s}\right) \tag{34}$$

The screened interaction matrix elements are given by:

$$W_{\alpha\beta} = -<\phi_\alpha\phi_\beta> + <\phi_\alpha><\phi_\beta> \tag{35}$$

We can first compute separately the $<\phi_\alpha>$ elements:

$$\begin{cases} <\phi_{ch}> = U^{ch}\dfrac{-2G_0}{1-(U^{ch}-3U^{sp})G_0^2} \\ <\vec{\phi}_{sp}> = 0 \end{cases} \tag{36}$$

$<\phi_{ch}>$ is related to the energy of charge interaction:

$$<\phi_{ch}> = U^{ch} < n > \tag{37}$$

$<\vec{\phi}_{sp}>$ is related to the energy of spin interaction:

$$<\vec{\phi}_{sp}> = 3U^{sp} < \vec{\sigma} > \tag{38}$$

it cancels here in the absence of symmetry breaking (no external field and no phase transition under 2D).
Let us now compute the non-connected bosonic propagator matrix elements. It is diagonal in channel indice.

$$\begin{aligned} -<\phi_{ch}\phi_{ch}> &= \frac{-1}{Z}\int D[\phi_{ch}]D[\vec{\phi}_{sp}]\phi_{ch}\phi_{ch}e^{-S(\phi,\bar{\varphi},\varphi)} \\ &= \frac{-1}{Z}\int D[\phi_{ch}]D[\vec{\phi}_{sp}]\exp\left(\frac{(U^{ch})^{-1}}{2}\phi_{ch}^2 + \frac{(U^{sp})^{-1}}{2}|\vec{\phi}_{sp}|^2\right)\left((G_0^{-1}+\phi_{ch})^2 - |\vec{\phi}_{sp}|^2\right)\phi_{ch}^2 \\ &= U^{ch}\frac{1-3(U^{ch}-U^{sp})G_0^2}{1-(U^{ch}-3U^{sp})G_0^2} \end{aligned} \tag{39}$$

$$-<|\vec{\phi}_{sp}|^2> = 3U^{sp}\frac{1-(U^{ch}-9U^{sp})G_0^2}{1-(U^{ch}-3U^{sp})G_0^2} \tag{40}$$

The full connected screened interaction is finally:

$$\begin{cases} W_{chch} = U^{ch}\left(\dfrac{1+3(U^{sp}-U^{ch})G_0^2}{1-(U^{ch}-3U^{sp})G_0^2} + 4\dfrac{U^{ch}G_0^2}{(1-(U^{ch}-3U^{sp})G_0^2)^2}\right) \\ W_{spsp,i} = U^{sp}\dfrac{1-(U^{ch}-9U^{sp})G_0^2}{1-(U^{ch}-3U^{sp})G_0^2} \end{cases} \tag{41}$$

4. Back to the initial problem

We have done the general computation and will now come back to the initial problem with the interaction $U\bar{\varphi}_\uparrow\varphi_\uparrow\bar{\varphi}_\downarrow\varphi_\downarrow$. This boils down to parametrize U^{ch} and U^{sp} from the condition $U = U^{ch} - 3U^{sp}$:

$$\begin{cases} U^{ch} = (3\alpha - 1)U \\ U^{sp} = (\alpha - 2/3)U \end{cases} \tag{42}$$

This gives us back the initial fermionic propagator:

$$G = \begin{pmatrix} \dfrac{G_0}{1 - UG_0^2} & 0 \\ 0 & \dfrac{G_0}{1 - UG_0^2} \end{pmatrix} \tag{43}$$

And the fully dressed interaction becomes:

$$W = \begin{pmatrix} (3\alpha - 1)U\left[\frac{1+(1-6\alpha)UG_0^2}{1-UG_0^2} + 4(3\alpha - 1)\frac{UG_0^2}{(1-UG_0^2)^2}\right] & 0 \\ 0 & (3\alpha - 2)U\frac{1+(6\alpha-5)UG_0^2}{1-UG_0^2} \end{pmatrix} \tag{44}$$

V. DRESSING PROCEDURE AND MULTIVALUEDNESS THROUGH A COMPLEX ANALYSIS VIEWPOINT

In this section we use complex analysis as a tool to explain and predict the multivaluedness occuring when dressing diagrams for the (0+0)d Hubbard model. Indeed, multivalued functions naturally appear in complex analysis when one wants to perform analytic continuations or when considering inverse functions of singular holomorphisms. We apply it to cases previously treated to revisit our understanding of the phenomenon in simple cases and to illustrate the idea.

A. General analysis

The starting point of this analysis is to remark that all physical quantities (Σ, G, Π, Γ ...) in the (0+0)d Hubbard model are analytical in U and G_0. This comes from the fact that they can be expressed with correlators, up to algebraic relations that conserve analyticity. Those correlators are by construction analytical in U and G_0. If moreover this physical quantity (noted f) is non-dimensionnal, then it is only a function of the variable UG_0^2. Here the term non-dimensionnal is abusive because our problem is already non-dimensionnal. Up to a multiplicative factor, we will assume that f always is a function of UG_0^2.

More generally, let us consider that f is a holomorphic function of n complex variables $u = (u_1, ..., u_n)$ that represent bare variables. Because it is holomorphic, it has a power series around each u. In particular, for $u = 0$ this is the bare diagrammatic series:

$$f(u) = \sum_{k_1,...,k_n} a_{k_1...k_n} u_1^{k_1} ... u_n^{k_n} \tag{45}$$

When using a bold formalism, we express our physical quantity in terms of n dressed variables $w = (w_1, ..., w_n)$. The skeleton series is the power series of f_{bold} around $w = 0$:

$$f_{bold}(w) = \sum_{k_1,...,k_n} b_{k_1...k_n} w_1^{k_1} ... w_n^{k_n} \tag{46}$$

We note B the dressing mapping : $B : u \mapsto w$. Let us consider $\tilde{f}$ a function of w on a domain $D_w = B(D_u)$ verifying $\tilde{f}(w) = \tilde{f}(B(u))$. The requirement for $\tilde{f}$ to be physical on this domain is that $\tilde{f}(B(u)) = f(u)$ for $u \in D_u$. In general, on an arbitrary domain of the w-space, when trying to find explicitly $\tilde{f}_{phys}(w)$, we implicitly invert the relation $\tilde{f}(B(u)) = f(u)$ which can have several solutions (branches) $\tilde{f}_i(w) = f\left(B_i^{-1}(w)\right)$ when B is not injective, and it requires choosing the physical branch.
The only constraint we have imposed to the skeleton series while dressing is to respect the bare series at each order in u which is a local requirement (local in the sense only near $u = 0$). This fixes the skeleton series to be the power series representation of the physical branch of $\tilde{f}_{phys}$ in a neighborhood of $u = 0$.

We can see here that the multivaluedness problem is contained in the structure of the dressing mapping B and its inverse. Here is given a useful theorem from complex analysis characterizing the multi-branching structure of B^{-1} given in the 1D case for sake of simplicity:

Let $B(u)$ be a holomorphic function on D and $u_0 \in D$ such that

$$B'(u_0) = B''(u_0) = ... = B^{(m-1)}(u_0) = 0,\ B^{(m)}(u_0) \neq 0, m \geq 2$$

Then there exists a neighborhood U of u_0 such that $W = B(U)$ is a neighborhood of $w_0 = B(u_0)$ and the mapping $B : z \mapsto w = B(u_0)$ is an m-to-1 mapping of $U \setminus \{u_0\}$ onto $W \setminus \{a\}$.

Where u_0 is a branching point where branches are equal (or "glued" together). A higher dimensionnal formulation can be found in [7]. More constrainted than functions of real variables (ex. $x \mapsto x^3$), singular functions of the complex variables are never injective which is the key point here.

In practice we can remember that if B is singular in u_0 (i.e $det\left(\frac{\partial w_i}{\partial u_j}\right) = 0$), $w_0 = B(u_0)$ is a branching point where at least two different branches of B^{-1} are glued together. All those points also define where the concerned branches B_i^{-1} are not analytical.

This property implies that evaluating $\tilde{f}$ using the same branch $\tilde{f}_i$ before and after the branching point cannot be physical as $f(u)$ is assumed to be analytical everywhere but none of the branches is. Recovering the whole physical $\tilde{f}$ thus requires knowing several branches while we only have informations about the one that is physical at weak correlation from the bold series.

Remark: Rigorously, this analysis is not complete to explain bold scheme failure at strong correlation. Indeed, at a branching point two branches are glued but nothing assures that the physical branch is involve. In practice we ommit this detail as the statement holds in all examples tried. This is still a powerful property to characterize physical and unphysical regimes and gives a mathematical interpretation to the branching phenomenon.

B. Examples

Because of expression 19, we are mainly interested in bold series for negative values of UG_0^2. Our previous analysis implies that singular points on the negative axis define the limit value of UG_0^2 beyond which the bold series is not physical anymore, as we try to evaluate it on a branch cut. We mean by evaluating the bold series with a bare variable u computing w(u) and then plugging it into the bold series.

1. UG^2-expansion

For the bold-G expansion, $u = UG_0^2$ and $w = UG^2$.

$$\begin{aligned} B : u \mapsto w &= \frac{u}{(1-u)^2} \\ B'(u) &= -\frac{1+u}{u-1} \end{aligned} \tag{47}$$

and B is singular for $UG_0^2 = -1$, the bold series is non viable beyond $UG_0^2 = -1$.

2. ΓG^2-expansion

For the fully dressed single and pair propagator formalism, $u = UG_0^2$ and $w = \Gamma G^2$.

$$\begin{aligned} B : u \mapsto w &= u\frac{1-2u}{(1-u)^3} \\ B'(u) &= -\frac{2u^2+2u-1}{(u-1)^4} \end{aligned} \tag{48}$$

and B is singular for $UG_0^2 = \frac{-1 \pm \sqrt{3}}{2}$, the bold series is non viable beyond $UG_0^2 = \frac{-1-\sqrt{3}}{2}$.

We see that finding skeleton series without branch cuts on the negative axis could allow to access arbitrary strong correlation regimes. This is what we attempt to do in the fully dressed formalism using Heisenberg decoupling.

VI. NUMERICAL RESULTS

The second dimension that we introduced do not allow us to fully analize the bold formalism computed in section IV. In this section we mainly used the module Sympy for symbolic caluclations and numpy for numerical.

A. Skeleton series

As the whole misleading convergence problem is contained in the inverting the dressing mapping B, let us take as a physical quantity of interest $u = u_{ch} - 3u_{sp}$, where $u_{ch} \equiv U^{sp}G_0^2$ and $u_{sp} \equiv U^{sp}G_0^2$. It is smooth in every variable which means that all errors of convergence we will observe only are due to the branching phenomenon.

The bare diagrammatic series coefficients of u is direct as it is a polynomial:

$$a_{1,0} = 1 \ , \ a_{0,1} = -3 \tag{49}$$

and all other coefficients are 0. In general, we used the python module Sympy to obtain our coefficients with symbolic calculations. We couldn't obtain the bold coefficients by inverting the dressing relation $(w_{ch}, w_{sp}) \equiv (W_{ch}G^2, W_{sp}G^2) = B(u_{ch}, u_{sp})$ and then power expanding u with respect to w_{ch} and w_{sp}. So we used the property of equivalence order by order in u-variables of the two series. The coefficients b_{nm} implicitly verify at each order N :

$$\sum_{n+m<N+1} b_{nm} w_{ch}^n(u) w_{sp}^m(u) - a_{nm} u_{ch}^n u_{sp}^m = o(u^{N+1}) \tag{50}$$

Which defines b_{nm} uniquely and amounts to inverting a linear system of N(N+1)/2 equations. We give here the coefficients up to order 6.

$b_{nm}^{(6)}$:

$$\begin{bmatrix} 0 & -3 & 0 & -81 & 648 & -10206 & 139968 \\ 1 & 12 & 45 & 540 & -1134 & 56376 & 0 \\ -4 & -63 & -396 & -4428 & -8424 & 0 & 0 \\ 19 & 324 & 2628 & 33264 & 0 & 0 & 0 \\ -92 & -1494 & -14256 & 0 & 0 & 0 & 0 \\ 426 & 5400 & 0 & 0 & 0 & 0 & 0 \\ -1768 & 0 & 0 & 0 & 0 & 0 & 0 \end{bmatrix}$$

Our algorithm takes 3 seconds for order 6. For order 26 it takes about 4 hours.

B. Singular points

The zero set of the Jacobian of $B(u_{ch}, u_{sp}) \mapsto (w_{ch}, w_{sp})$ is given by the zeros of its numerator:

$$\begin{aligned} &3u_{ch}^4 - 72u_{ch}^3 u_{sp} + 6u_{ch}^3 + 378u_{ch}^2 u_{sp}^2 - 126u_{ch}^2 u_{sp} - 6u_{ch}^2 - 648u_{ch}u_{sp}^3 \\ &+162u_{ch}u_{sp}^2 - 24u_{ch}u_{sp} - 2u_{ch} + 243u_{sp}^4 + 54u_{sp}^3 - 54u_{sp}^2 - 18u_{sp} - 1 \end{aligned} \tag{51}$$

This set defines where the differents branches of B^{-1} are glued together. It is impossible to represent this set that has for complex dimension 1 (2 real dimensions) in a 2D complex dimension space (4 real dimensions). We give a plot of it when restricting to real values (Fig. 3).

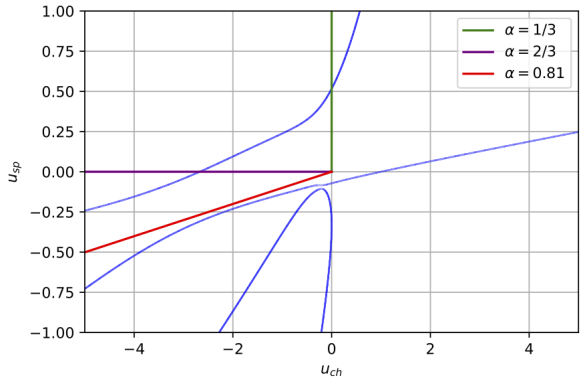

Figure 3. In blue, the real slice of the set of branching points where B^{-1}'s branches join. This set is a 1 real dimensional manifold as being the real slice of a 1 complex dimensional analytical set. In other colors, the paths when UG_0^2 goes from 0 to $-\infty$ for different values of α.

We can already see for real values that the structure of this zero set is non trivial. For values of alpha between ≈ 0.76 and ≈ 0.84, there is no singular points at all on the negative real axis of u. This means for those values of alpha that one remains on the same branch along the path $u = 0$ to $u = -\infty$ which is promising to access high correlation. Because this set of alpha is an interval (so it is dense), there should be a dense class of conformal maps allowing to access arbitrary high values of correlation. However in 4D our topological understanding is limited. Moreover, another phenomenon is limiting in practice as we will see for the case $\alpha = 2/3$. Two cases are of particular interest. For $\alpha = 1/3$, $u_{ch} = w_{ch} = 0$ and for $\alpha = 2/3$, $u_{sp} = w_{sp} = 0$ which reduces the dimensionality to 1 in those two particular cases.

C. Case $\alpha = 1/3$

For $\alpha = 1/3$, $u_{sp} = -u/3$, $u_{ch} = 0$ and $B : u \mapsto w = u\dfrac{3u-1}{3(1-u)^3}$. Its singular points in the u-plane and w-plane are plotted below (Fig. 4). We also plot numerically (Fig. 5) the bold truncated series, Dlog-pade extrapolation of the bold truncated series, and their relative error to u. For Dlog-pade technique, at order N and noting $m = integer(N/2)$ and $n = N - m$, we averaged results for orders $(m-2, n+2), (m-1, n+1), (m, n), (m+1, n-1)$ and $(m+2, n-2)$. The branching point on the negative axis is at $u = -\dfrac{2+\sqrt{7}}{3} \approx -1.55$.

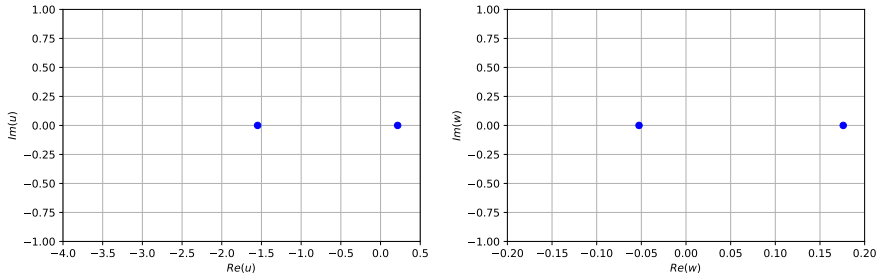

Figure 4. Branching points in the u-plane (left) and the w-plane (right), for $\alpha = 1/3$.

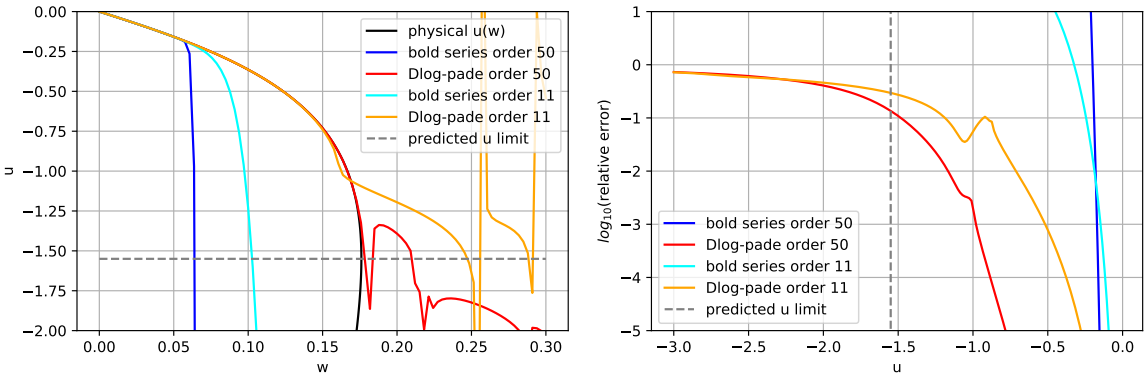

Figure 5. On the left, two different numerical schemes to attempt recovering u(w). On the right, log_{10}(relative error). For alpha $= 1/3$.

D. Case $\alpha = 2/3$

For $\alpha = 2/3$, $u_{ch} = u$, $u_{sp} = 0$ and $B : u \mapsto w = u\left(\frac{1-3u}{(1-u)^3} + 4\frac{u}{(1-u)^4}\right)$. As for the case $\alpha = 1/3$, we plot singular points (Fig. 6), the comparison of truncated series and Dlog-pade extrapolation, and the relative error (Fig. 7).

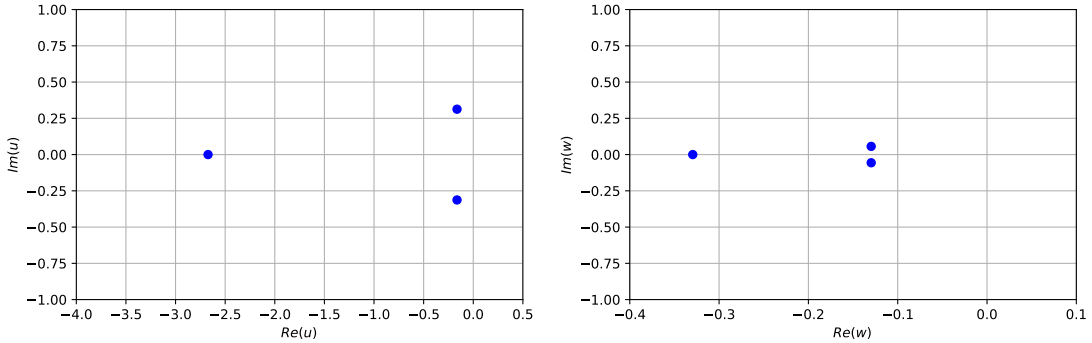

Figure 6. Branching points for $\alpha = 2/3$.

The branching point on the negative axis is at $u \approx -2.67$. In this case, we observe that Dlog-pade extrapolation

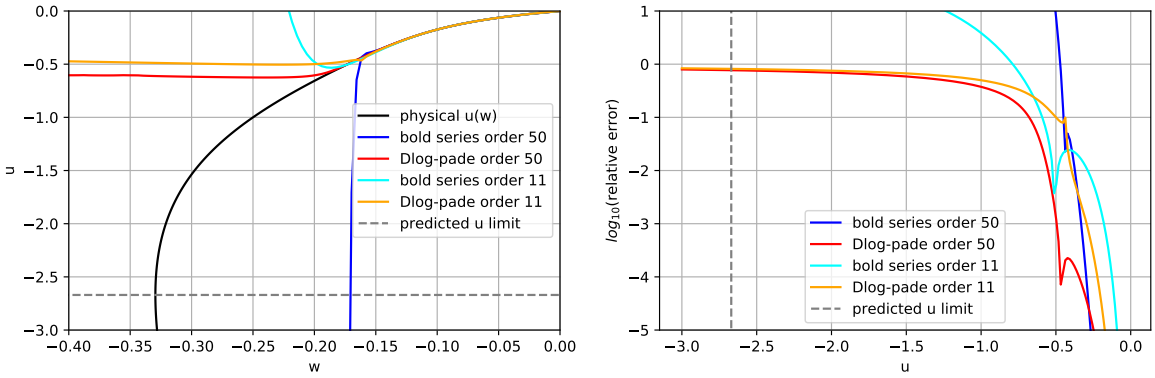

Figure 7. On the left, two different numerical schemes to attempt recovering u(w). On the right, log_{10}(relative error). For alpha = 2/3.

fails very quickly compared to what happens for $\alpha = 1/3$. Indeed, the extrapolation is done on the basis of the bold truncated series. Which means that our algorithm aims to extrapolate the series beyond the two conjugated singularities in the w-plane. Those latter are very close to the real axis and because of this proximity, the analysis shows that our extrapolation algorithm constructs a spurious singularity on the real axis nearby. We also have tried to remove those two branch with conformal maps but with no significant improvement. The problem of the conformal mapping technique is that it won't be suitable for general α. We are thus confronted to a numerical limit that implies a bad convergence of the technique for $\alpha = 2/3$.

E. General α

We only used numerical techniques for 1D-series. There is however arbitrariness when deciding how to convert our 2D-partial sum into a 1D array to give to extrapolation algorithms. The general method, for a given parameter (α, u), is to parametrize the 2D sum with only one parameter ω:

$$\sum_{n+m<N+1} b_{nm} w_{ch}^n(u) w_{sp}^m(u) \xi_{ch}^n(\omega) \xi_{sp}^m(\omega) = \sum_{k<N+1} c_k(\xi_{ch}, \xi_{sp}) \omega^k + O(\omega^{N+1}) \tag{52}$$

where ξ_{ch} and ξ_{sp} are holomorphisms of ω and verify $\xi_{ch}(1) = \xi_{sp}(1) = 1$ such that the truncated 1D series in ω is equal to the physical 2D series when $\omega = 1$. In results below (Fig. 8), pade or Dlog-pade extrapolations have been done for $\xi_{ch}(\omega) = \xi_{sp}(\omega) = \omega$.

We remark lots of numerical instabilities of the Dlog-pade technique that are probably artefacts. We thus added the result for standard pade extrapolation technique. On the whole, we see that the range of validity has indeed been improved thanks to this fully-bold formalism, but knowing how it evolves with α is not trivial.

CONCLUSION

The fully-bold formalism for decoupled charge and 3D spin channels for the (0+0)d Hubbard model shows a very rich behavior of physical and unphysical regime. We have shown that this formalism had promising results with respect to its range of physicalness. The extra dimension introduced and encoded in the parameter α non-trivially influences this range of validity. This can be due to the Hubbard-Stratonovic transformation which is a non-linear transformation. The fact that some tunings of α predict no branch switching for arbitrary strong correlation is a promising result. However because of this multidimensionality the analysis and full resolution of the problem

is hard. Moreover we are numerically limited and considering arbitrary high orders would be irrelevant as we are limited to order 10 with physical diagrammatic Monte Carlo. Of course, it is hard to transpose this result to physical problems and an implementation of this formalism for the Hubbard atom would be a great complement to this study. Another question is wether, as for the Hubbard atom and the (0+0)d Hubbard model, the (1+0)d electron-boson problem can be modelled by its (0+0)d equivalent.

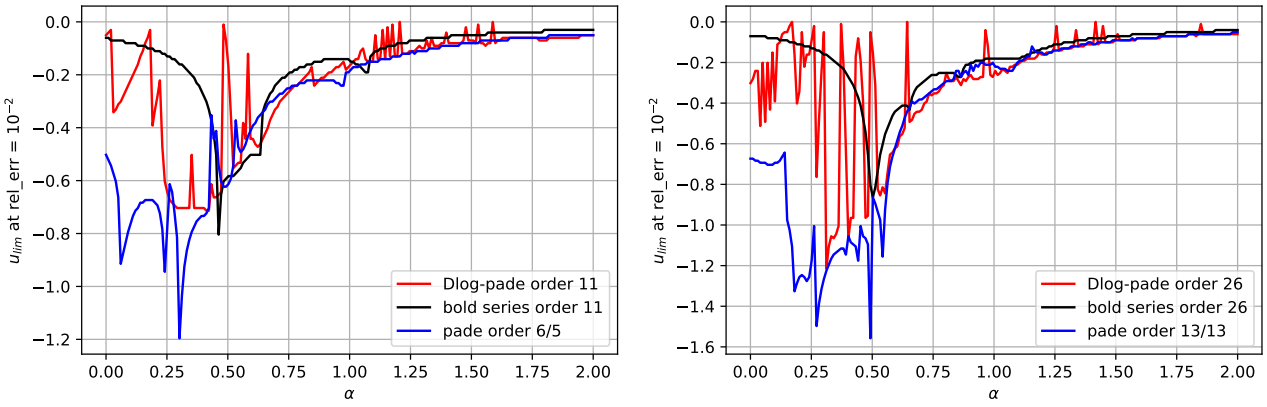

Figure 8. Plots of the u limit such that the bold series has relative error inferior to 10^{-2} in function of alpha, for orders 11 and 26.

[1] Thomas Ayral and Olivier Parcollet. Mott physics and spin fluctuations: A functional viewpoint. *Physical Review B*, 93(23), jun 2016.

[2] A. L. Fetter and J. D. Walecka. *Quantum Theory of Many-Particle Systems*. McGraw-Hill, Boston, 1971.

[3] Richard Phillips Feynman and Albert Roach Hibbs. *Quantum mechanics and path integrals*. International series in pure and applied physics. McGraw-Hill, New York, NY, 1965.

[4] Aaram J. Kim and Vincent Sacksteder. Multivaluedness of the luttinger-ward functional in the fermionic and bosonic system with replicas. *Phys. Rev. B*, 101:115146, Mar 2020.

[5] Evgeny Kozik, Michel Ferrero, and Antoine Georges. Nonexistence of the luttinger-ward functional and misleading convergence of skeleton diagrammatic series for hubbard-like models. *Physical Review Letters*, 114(15), apr 2015.

[6] John W. Negele and Henri Orland. *Quantum Many-particle Systems*. Westview Press, November 1998.

[7] R.M. Range. *Holomorphic Functions and Integral Representations in Several Complex Variables*. Graduate texts in mathematics. Springer, 1986.

[8] Riccardo Rossi and Félix Werner. Skeleton series and multivaluedness of the self-energy functional in zero space-time dimensions. *Journal of Physics A: Mathematical and Theoretical*, 48(48):485202, oct 2015.

[9] M.S. Swanson. *Path Integrals and Quantum Processes*. Dover Books on Physics. Dover Publications, 2014.

[10] K. Van Houcke, E. Kozik, R. Rossi, Y. Deng, and F. Werner. Physical and unphysical regimes of self-consistent many-body perturbation theory, 2021.

Acknowlegement

Many thanks to my supervisor Evgeny Kozik for those interesting discussions!